

## Original Research Article

# STRUCTURAL AND OPTO-ELECTRICAL PROPERTIES OF CUPROUS OXIDE THIN FILM PREPARED BY THERMAL OXIDATION TECHNIQUE

---

### ABSTRACT

**Aim:** The structural, morphological and opto-electrical characteristics of cuprous oxide produced by thermal oxidation are investigated in this study.

**Methodology:** Thermal oxidation of copper foils was used to develop high-quality cuprous oxide crystals, and the process proved to be effective in producing cuprous oxide films with high purity and big grain size.

**Results:** X-ray diffraction (XRD) analysis revealed the film's cubic structure. Large peaks in the XRD patterns indicate that the produced films were made up of a single  $\text{Cu}_2\text{O}$  phase with no interstitial phase and a nano-grain structure with a preferred (111) orientation at  $2\theta$  angle of  $36.51^\circ$ . The mean crystallite size calculated using the Debye Scherrer model was found to be 26nm. Scanning electron microscope (SEM) revealed that the material is rough on a microscale, and the average grain size for the crystal was estimated to be  $0.68\mu\text{m}$ . There were reflections of crystal defects such as vacancies and dislocation due to the process of annealing. The room temperature optical absorption coefficient was analysed using transmission spectra data where the optical band gap energy was found to be 2.11eV.

**Conclusion:** The findings are important in applications in semi-conductor devices such as solar cells, optical sources and detectors.

*Keywords: Cuprous oxide, Thermal oxidation, Characterization, Solar cell, X-ray diffraction (XRD), Scanning electron microscope (SEM)*

### 1. INTRODUCTION

Copper's superior electrical conductivity and low-cost manufacture make it ideal for a wide range of electronic applications. Copper's usage in nanoelectronics is limited by two main issues: i) its diffusivity and (ii) easy oxidation, even in vacuum. [1]. The key features of  $\text{Cu}_2\text{O}$  that makes it attractive are: it is environmentally friendly and affordable due to its lack of toxicity. It's also easy to come by and plentiful. Similarly, factors such as tuning the particle size can easily change the band gap of  $\text{Cu}_2\text{O}$ . [2]. Various methods were used to prepare cuprous oxide nanoparticles such as electrodeposition [3], thermal oxidation [4] and so on.

[5] used RF sputtering to create high-quality copper dioxide ( $\text{Cu}_2\text{O}$ ) and copper oxide ( $\text{CuO}$ ) thin films and investigate the impact of thermal oxidation on their physical properties for optoelectronic applications. [5]. [6] used thermal oxidation to make cupric oxide nanowires and investigated their electrical characteristics. [6]. [7] synthesized cuprous oxide by a simple wet-chemical process, and its physical characterisation was obtained for biomedical diagnosis, carriers in drug-delivery agents, and cell imaging, [7].

As synthesized,  $\text{Cu}_2\text{O}$  is a P-type semi-conductor with a band gap of 2eV and has been considered as a potential of light absorbing material in solar cells [8]. Cuprous oxide was produced due to its non-toxicity, environmental acceptability, availability and costly affordable via thermal oxidation technique in this work. Samples were analysed using XRD, SEM, UV-VIS and four point resistivity probe method.

## 2. EXPERIMENTAL PROCEDURE

### 2.1 SAMPLE PREPARATIONS

The surface of high purity copper foil (thickness 0.1mm, industrial grade 99.00 percent) was properly cleaned and smoothed with the end of a beaker, then polished to remove any grease or dirt. It was then plunged for two minutes in a 30 percent nitric acid ( $\text{HNO}_3$ )<sub>2</sub> solution. It was cut into regular sizes of 2cmx2cm, washed in deionized water before being dried using tissue paper. [9].

### 2.2 THERMAL OXIDATION

Thermal oxidation was carried out at atmospheric pressure in a Gallen Kamp type M1220 high temperature furnace. The temperature was kept constant at 950°C. The samples were held in a ceramic crucible. With the help of tongs, the sample was placed into the furnace after the oxidation temperature was reached. To begin the oxidation time count, the furnace door was closed and the stop clock was activated. The sample was brought out and quickly quenched in cold deionized water to stop further oxidation as soon as the oxidation time reached 5 minutes. At the same temperature and for different times (950/7mins and 950/9mins), the process was repeated for the remaining samples. This was done to determine the optimal oxidation time, after which the best oxidized sample was chosen [10]. To prevent additional oxidation, the samples were quickly quenched in distilled water. The samples were heat treated (annealed) in a furnace for 1 1/2 hours at a lowered temperature of 500°C. This was accomplished by heating the samples to 500°C in a furnace (Gallen Kamp model no. M1220) and leaving them there for 1 1/2 hours before quenching them in cold deionized water. The samples were then immersed in a solution containing 10 grams of  $\text{FeCl}_2$ , 8 grams of  $\text{NaCl}$  dissolved in 200 millilitres of deionized water, and 40 cm<sup>3</sup> of concentrated  $\text{HCl}$ . It was shook for 4 minutes till the colour of  $\text{Cu}_2\text{O}$  turned reddish-brown. To stop the etchant from acting any further, the samples were dipped in a solution containing 10 grams of sodium per sulphate ( $\text{Na}_2\text{S}_2\text{O}_8$ ) dissolved in 250mls of deionized water, and then cleaned in deionized water. The samples were then immersed in a solution comprising 100cm<sup>3</sup> of concentrated nitric acid ( $\text{HNO}_3$ ) and 2 grams of  $\text{NaCl}$  to remove the copper (I) oxide ( $\text{Cu}_2\text{O}$ ) layer from one side before being dipped in a solution containing 5 grams of sodium per sulphate in 100cm<sup>3</sup> deionized water. After that, the samples were rinsed with deionized water and dried. [9].

### 2.3 RESISTIVITY MEASUREMENT.

Resistivity measurement was carried out on copper (I) oxide samples which were initially thermally oxidized in laboratory air while some were oxidized in the presence of  $\text{HCl}$  vapour. Measurements were made on both annealed and un-annealed samples using the collinear four-probe [11]. Some samples were given heat treatment (annealing) at 500°C and then etched before measurements were taken. The resistivity value ( $\rho$ ) was calculated using inverse of the slope and the thickness (t) of the copper (I) oxide layer.

### 2.4. CHARACTERISATION DETAILS

The structural properties of the prepared specimen were examined using the X-ray diffraction system (operating at 40 kV and 40 mA, using  $\text{Cu-K}\alpha$  radiation collected at 20°-80° with phase size 0.01°. Bruker AXS D8 advance diffractometer). The surface morphology and micro structure of copper foil and layer were observed using the scanning

electron microscope (SEM) model (ProX): phenom world: 800-0733, and the electrical resistivity of the semiconductor material was measured using the four point probe device.

### 3. RESULTS AND DISCUSSION

#### 3.1 THE XRD ANALYSIS

The XRD patterns of the samples revealed five  $\text{Cu}_2\text{O}$  peaks with  $2\theta$  values of  $29.51^\circ$ ,  $36.51^\circ$ ,  $42.39^\circ$ ,  $61.50^\circ$ ,  $73.56^\circ$ , and  $77.44^\circ$ , respectively, corresponding to the crystal planes of (110), (111), (200), (220), and (311). All of the peaks in the XRD patterns agree with the standard data in the power diffraction file (PDF) phase identification value 050667, indicating that the  $\text{Cu}_2\text{O}$  cubic crystal structure is present. There are no more phases that have been discovered.  $\text{Cu}_2\text{O}$  reflects prominently along the (111) plane at a  $2\theta$  angle of  $36.51^\circ$ . The five peaks in the XRD spectrum matched the results provided by in a good way [12][13]. The crystal size of the particle was calculated using Scherrer's formula equation (1) and found to be 26.6nm, which agrees well with [2] findings, and the lattice parameter of  $\text{Cu}_2\text{O}$  was calculated using equation (2) and found to be 0.4257nm, which agrees well with [14].

$$D = \left( \frac{0.94\lambda}{\beta \cos \theta} \right) \quad (1)$$

$$a = d_{hkl} \sqrt{h^2 + k^2 + l^2} \quad (2)$$

With  $\lambda$  as the wavelength of X-rays, having a value of 1.54059Å,  $\beta$  is the full width at half the maximum and  $\theta$  is the diffraction angle of the Bragg, h, k, l is the Miller indices and  $d_{hkl}$  as the inter-planar spacing.

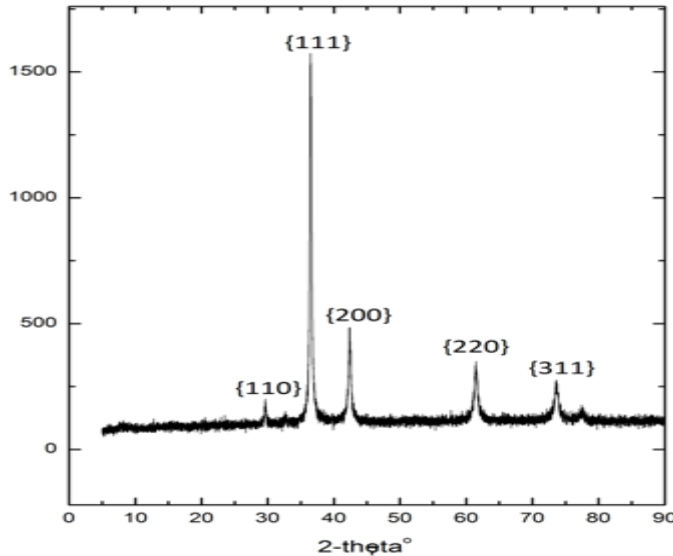
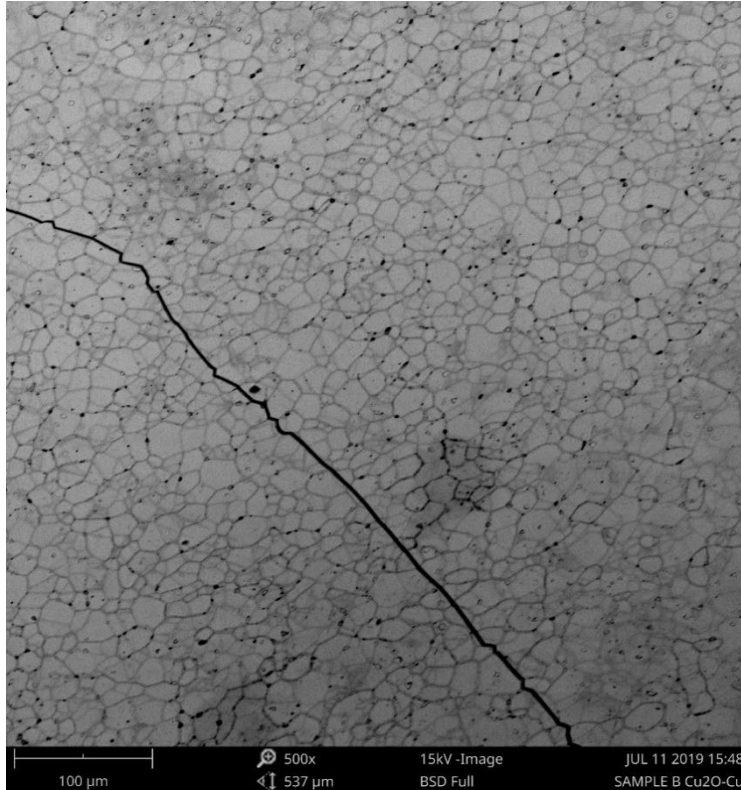


Fig. 1 XRD spectra of  $\text{Cu}_2\text{O}$

#### 3.2 THE MORPHOLOGY ANALYSIS

The scanning electron microscope (SEM) model (ProX): phenom world: 800-0733 at Ahmadu Bello University Zaria (Chemical Engineering Department), was used to examine the surface morphology and microstructure of copper foil layer. SEM micrographs depict the surface morphology and crystallinity of copper (I) oxide that was oxidized at  $950^\circ\text{C}$  for 5 minutes and then annealed at  $500^\circ\text{C}$  for 90 minutes, revealing the compactness and smooth grain structure.  $\text{Cu}_2\text{O}$  micrographs look darker due to the dense nature of crystal formation as a result of the annealing process, as well as the creation of black  $\text{CuO}$  on top of the red layered  $\text{Cu}_2\text{O}$ , which was later removed by etching. The grains in the micrograph are nearly similar in size, and the gaps between them could be the product of inadequate grain

development after the oxidation process. The number of grain boundaries has also been discovered to increase when grain size decreases. The dark areas of the micrograph are spots where the surface crystals were removed for the first time [15]. On both sides of the grain boundaries (an essential location in polycrystalline solar material), an electrostatic barrier forms, which blocks the bulk of carrier fluxes and acts as a huge series resistance. The average grain size of the  $\text{Cu}_2\text{O}$  sample crystals was calculated to be  $0.68 \mu\text{m}$ .



**Fig. 2. scanning electron microscope (SEM) model image**

### 3.3 OPTICAL MEASUREMENT ANALYSIS

The Tauc's plot of the UV-Vis spectra graph of  $(ah\nu)^2$  against  $(h\nu)$  were plotted for  $\text{Cu}_2\text{O}$ . Developing the electronic band structure of a nanomaterial frequently necessitates determining the band gap energy ( $E_g$ ). The band gap energy of  $\text{Cu}_2\text{O}$  was found to be 2.11eV, as shown in the graph (figure 3), which is in concord with previous results [14][16][17][2]. This demonstrates that  $\text{Cu}_2\text{O}$  particles are photoelectrically active when exposed to visible light [2].

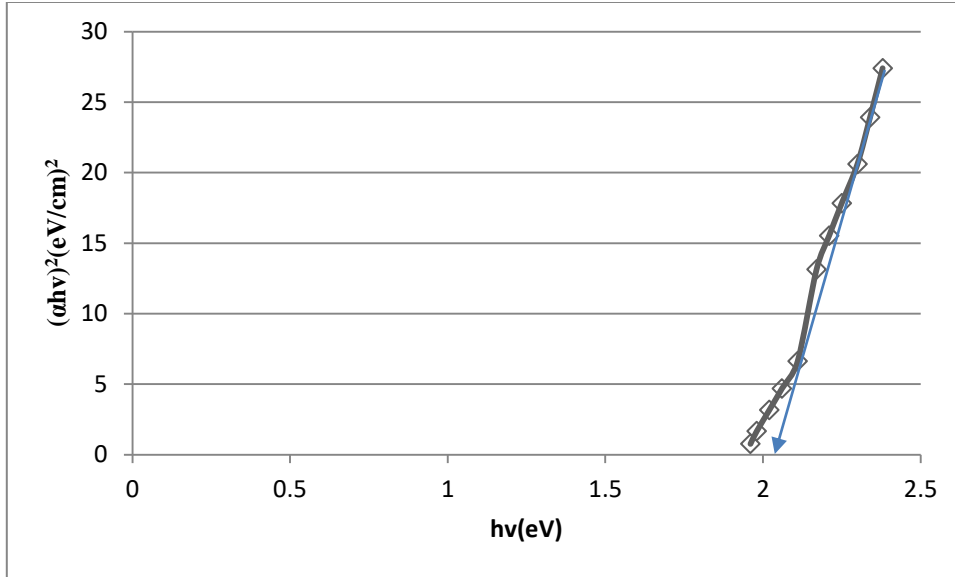


Fig. 3. Optical measurement analysis

### 3.4 RESISTIVITY MEASUREMENT ANALYSIS

The sample oxidized in the presence of HCl vapour and further annealed give the best resistivity value of  $2.59 \times 10^2 \Omega\text{cm}$  which shows a significant decrease in the resistivity value when compared to the value found for the sample not oxidized in the presence of HCl vapour. The lower resistivity value of  $\text{Cu}_2\text{O}$  is ascribed to chlorine [15] [18]. The resistivity has been calculated by [19][20] using the expression for resistivity given by equation (3).

$$\rho = \frac{\pi}{\ln 2} \left( \frac{V}{I} \right) t = 4.532 \left( \frac{V}{I} \right) t \quad (3)$$

Where V is voltage between the inner probes, I the Current through the outer probes, and, t is the sample thickness. From the graph of I-V (figure 4) plot for  $\text{Cu}_2\text{O}$ , the electrical resistivity of  $\text{Cu}_2\text{O}$  was calculated to be  $2.59 \times 10^2 \Omega\text{cm}$ , which is also in good agreement with the reports of [21].

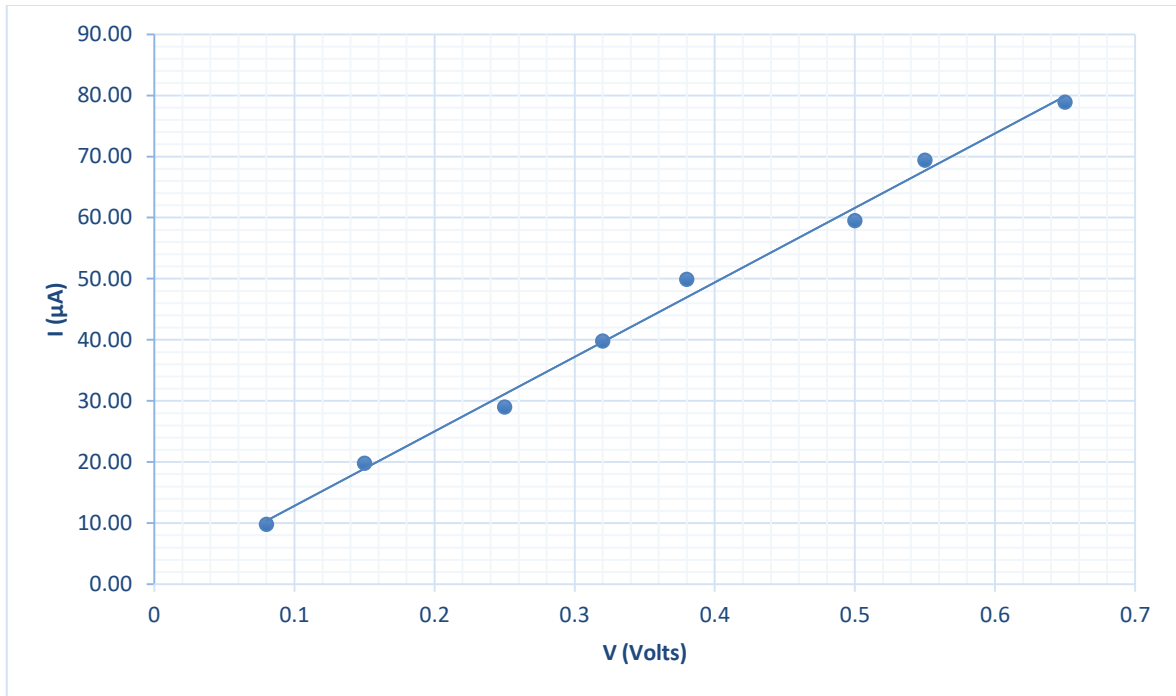


**Figure 4 : A graph of current versus voltage.**

#### **4. CONCLUSION**

Cuprous oxide was successfully synthesized via thermal oxidation technique, XRD analysis indicate that the produced films are made up of a single  $\text{Cu}_2\text{O}$  phase with no interstitial phase and a nano-grain cubic structure with a preferred (111) orientation at  $2\theta$  angle of  $36.51^\circ$  and crystal size of 26.6nm. SEM micrograph reveals that the material is rough on a micro-scale with an average grain size of  $0.68\mu\text{m}$ , while the room temperature optical absorption coefficient was analysed using transmission spectra data, and the optical band gap energy was estimated to be around 2.11eV. The low electrical resistivity of  $2.59 \times 10^2 \Omega\text{cm}$  was calculated for  $\text{Cu}_2\text{O}$  which makes it a good candidate for photovoltaic applications.

## COMPETING INTERESTS DISCLAIMER:

**AUTHORS HAVE DECLARED THAT NO COMPETING INTERESTS EXIST. THE PRODUCTS USED FOR THIS RESEARCH ARE COMMONLY AND PREDOMINANTLY USE PRODUCTS IN OUR AREA OF RESEARCH AND COUNTRY. THERE IS ABSOLUTELY NO CONFLICT OF INTEREST BETWEEN THE AUTHORS AND PRODUCERS OF THE PRODUCTS BECAUSE WE DO NOT INTEND TO USE THESE PRODUCTS AS AN AVENUE FOR ANY LITIGATION BUT FOR THE ADVANCEMENT OF KNOWLEDGE. ALSO, THE RESEARCH WAS NOT FUNDED BY THE PRODUCING COMPANY RATHER IT WAS FUNDED BY PERSONAL EFFORTS OF THE AUTHORS.**

## REFERENCES

- [1] L. De Los Santos Valladares *et al.*, (2012). Crystallization and electrical resistivity of Cu<sub>2</sub>O and CuO obtained by thermal oxidation of Cu thin films on SiO<sub>2</sub>/Si substrates. *Journal of Thin Solid Films*, 520 (2012) 6368–6374
- [2] Huang *et al.*, (2008). Preparation of cuprous oxides with different sizes and their behaviours of adsorption, visible-light driven photocatalysis and photo corrosion. *Solid State Sciences* 11 (2009) 129-138
- [3] Siripala *et al.*, (1996). Study of annealing effects of cuprous oxide grown by electrodeposition technique. *Solar energy materials and solar cells* vol. 44, 251-260
- [4] Liang *et al.*, (2010). Cross-sectional characterization of cupric oxide nanowires grown by thermal oxidation of copper foils. *Applied Surface Science* 257 (2010) 62–66
- [5] Makrami *et al.*, (2018). Thermal oxidation effects on physical properties of CuO<sub>2</sub> thin films for optoelectronic application. *Materials Research Express* vol 2053:1591
- [6] Gonclaves, A.M.B., Campos, L.C., Ferlauto, A.S. and Lacerda, R.G. (2009). On the growth of electrical characterization of CuO nanowires by thermal oxidation. *Journal of applied physics*, **106**: 034303-(1-5).
- [7] Ning *et al.*, (2010). Room temperature preparation of cuprous oxide hollow microspheres by a facile wet-chemical approach. *Applied Surface Science* 256 (2010) 7335–7338
- [8] Eray, S. Aydil, Advisor (2010). Thin Zinc oxide and cuprous oxide films for photovoltaic application. (Unpublished Ph.D. thesis).
- [9] Ohajianya, A.C., and Abumere, O. E. (2013). Effect of Cuprous oxide (Cu<sub>2</sub>O) film thickness on the efficiency of the copper-cuprous oxide (Cu<sub>2</sub>O/Cu) Solar cell. *The Internal journal of engineering and Science (IJES)* **2**(5):42-47.
- [10] Abdu, Y. and Musa, A. O. (2009). Copper (I) oxide (Cu<sub>2</sub>O) based solar cells-A review. *Bayero journal of pure and applied sciences*, **2**(2): 8-12.

- [11] Dieter, K.S. (2006): Semiconductor material and device characteristic. *John Wiley and Sons*
- [12] Huiling, L., Yongen, L., Ying, H., Yueping, F., Yuehua, X., Li, Z. and Xin, L. (2011). Photocatalytic reduction of carbon dioxide to methanol by  $\text{Cu}_2\text{O}$  /sic nanocrystallite Under visible light irradiation. *Journal of Natural gas chemistry*, **20**(2011):147-148.
- [13] Juan Wang, Yajiang Li, Peng Liu and Haoran Geng (2008). Microstructure and XRD analysis in the interface zone of Mg/Al diffusion bonding. *Journal of Materials Processing Technology* **205**(1-3): 146-150.
- [14] Katayama, J., Ito, K., Matsuoka, M., Tamaki, K. (2004). Performance  $\text{Cu}_2\text{O}/\text{ZnO}$  solar cell prepared by two step electrodeposition. *Journal of Applied Electrochemistry*, **34**:687-692.
- [15] Musa, A. O. (1995). *Development of Thin Film Copper (I) oxide for Backwall Schottky Barrier Solar Cells*. University of Ilorin Ph.D Thesis.
- [17] Bessekhoud, Y., Robert, D., Weber, J.V. (2005). *Catal Today*, **101**:3-4.
- [18] Onimisi, M.Y., Hariharan, N and Musa, A.O (2007). Effect of oxidation temperature and oxidation time on thickness of copper (I) oxide ( $\text{Cu}_2\text{O}$ ) solar cell. *Nigerian Journal of Physics* **19**(1).
- [19] Valdes, L.B. (1954). *Proc. IRE*, **42**:420
- [20] Onimisi, M. Y. (2008). Effects of annealing on the resistivity of Copper (I) oxide solar cells. *International journal of physical sciences*. **3**(8):194-196.
- [21] Farhad *et al.*, (2020). Pulsed laser deposition of single-phase n- and p-type  $\text{Cu}_2\text{O}$  thin films with low resistivity. *Materials and Design* **193** (2020) 1088-48